1

Volume 12
February 2019, 44–54
ISSN 1867-0520

Reprint

Steel Construction

Design and Research

Transfer of shear stresses at steel-concrete interface – Experimental tests and literature review

Maciej Chrzanowski
Christoph Odenbreit
Renata Obiala
Teodora Bogdan
Hervé Degée

Ernst & Sohn
A Wiley Brand

ECCS
CECM
E K S

DOI: 10.1002/stco.201800024

Maciej Chrzanowski*, Christoph Odenbreit, Renata Obiala, Teodora Bogdan, Hervé Degée PAPER

Transfer of shear stresses at steel-concrete interface

Experimental tests and literature review

Shear stresses can be transferred via bond at the steel-concrete interface without having to consider any mechanical shear connectors. The research conducted shows that the use of anti-adhesive products, such as grease, reduce the bond at the steel-concrete interface in push-out tests (POTs). However, the effect is still significant, especially for fully encased steel profiles. The results of an experimental POT campaign with nine small-scale cube specimens and two composite column specimens are presented here. Three different surface conditions were examined: a) an untreated surface, b) a surface treated with anti-adhesive agent (formwork release oil) and c) a surface treated with PTFE spray. The resulting ultimate shear stresses were compared with the experimental results available in the literature [1–10]. How the different geometries of the specimens, the concrete age and the surface treatment conditions influence the bond strength are compared and summarized.

Keywords: steel-concrete composite columns; composite action; longitudinal shear; steel-concrete bond; shear stresses between plain steel and concrete surfaces; assessment of steel-concrete bond strength; analysis of steel-concrete bond behaviour

1 Introduction

Tall buildings are rising higher and higher and the structural members of such buildings have to resist increasing forces. The technology allowing such developments is evolving faster than the design standards and codes. The research presented here focuses on composite columns. Heavy vertical members are the backbone of every tall building and their design goes far beyond the state of the current design codes. For example, the current EN 1994-1-1 [11] provides for cross-sections with only one steel section and double symmetry. In the meantime, heavy composite column members with multiple, separately encased steel profiles are in use in many buildings around the world (see Fig. 1). Typically, the force transfer between the steel profile and the concrete, which ensures composite action, is achieved by mechanical shear connectors, mostly shear studs.

Various mechanical shear connectors are used to transfer the shear forces between the steel and concrete load-bearing elements of composite columns. The load-bearing capacity of these connectors can be determined in laboratory tests, e.g. the push-out test (POT). The measured shear resistance of the connection consists of the mechanical part and the bond at the interface between the materials. It has been concluded that for the analytical evaluation of test results and an understanding of the long-term behaviour of the connection, it is important to distinguish between the part of the load that is transferred by the mechanical shear connector and the part that is transferred by direct bond between the concrete and steel surfaces.

The focus in this research was to identify the resistance of the mechanical shear connector that was recently developed by Chrzanowski et al. [12], see Fig. 1b. Therefore, the layout of the structural test had to be designed in a way that the shear force transfer by the bond is minimised by an appropriate surface treatment. It is common practice to ignore the steel-concrete bond in the experimental testing of shear connectors by applying grease. However, based on this assumption, the load-bearing capacity and initial stiffness of the mechanical shear connectors, especially for push-out type tests on columns with fully in concrete embedded steel profiles, might be overestimated. After greasing the steel profile, the bond at the interface is reduced, but it is not equal to zero and its contribution to the force transfer mechanism may still be significant [13]. Consequently, a number of tests have been performed to evaluate the pure steel-concrete bond strength without any mechanical shear connection. An accurate evaluation of the forces transferred by bond allows a better insight into the mechanical connection mechanism and a better assessment of its resistance [12], [13].

As will be shown later, it is impossible to eliminate the bond fully. Therefore, for the later test evaluation, it is in-

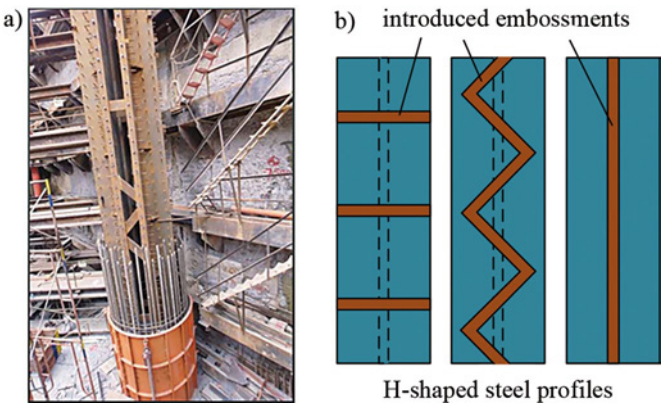

Fig. 1. Shear connections in composite columns: a) construction detail of IFC Tower 2, Hong Kong (source: Raymond Wong) and b) the concept investigated in terms of optimizing the mechanical shear connection [12]

*) Corresponding author: maciej.chrzanowski@uni.lu
Submitted for review: 25 September 2018
Accepted for publication: 28 November 2018

dispensable to know that part of the shear force that is transferred by bond. Shear forces due to bond at the steel-concrete interface are transferred by two phenomena: i) chemical adhesion and ii) friction. Within the friction phenomenon itself, it is necessary to distinguish between two major mechanisms: a) Coulomb friction and b) surface roughness friction. Activation of Coulomb friction requires always a normal force acting perpendicular to a surface, whereas surface roughness friction can be activated without any external pressure when two sliding surfaces are in contact. This effect has been investigated by Goralski [14] and others.

2 Test campaign overview

Nine small-scale cube push-out tests (SSCPOTs) and two column-type push-out tests (CoPOTs) were performed within a test campaign of the MultiCoSteel research project in the engineering structures laboratory of the University of Luxembourg, see Table 1. Both test series used the same type of specimen, where the steel part was fully embedded in the concrete block. The SSCPOT series incorporated three different surface treatment conditions in order to analyse the reduction in shear stresses due to the different bond-reducing products applied. In addition, no concrete confinement was introduced in the form of reinforcing bars. The CoPOT series investigated only specimens with surfaces treated with release agent oil, and included a reinforcement cage. There was a recess at the bottom of each specimen in order to allow a free downward slide of the steel part, see Figs. 2 and 3. In both test series, the embedded steel parts were not subjected to any cleaning processes and used in the specimens in the state 'as delivered', including the surfaces imperfections created during the milling process.

2.1 Geometry and material properties of small-scale cube push-out tests

The SSCPOT experimental test series comprised nine specimens with nominally identical geometry and material properties. The specimens only varied in terms of the steel surface treatment conditions: untreated (PS), greased with oil (G) and Teflon-coated (PTFE). The test specimens were composed of two parts: a concrete cube with dimensions of 150 × 150 × 150 mm and an embedded steel bar with a rectangular cross-section measuring 10 × 30 mm and a length of 150 mm. The embedded length of the steel bar was 100 mm. The steel bars used had been cut from one longer steel bar. The geometry of the specimen is shown in Fig. 2.

The material properties of the test specimens were based on the normative values for S235JR steel according to EN 10025-1:2004 [15] and for C35/45 concrete according to EN 206-1:2000 [16] given on the concrete supplier's certificate, received upon delivery. The age of the concrete upon testing was 21 days.

2.2 Geometry and material properties of column push-out tests

In the CoPOT series, two nominally identical test specimens were fabricated and tested. The specimens contained a centrally embedded HEB120 steel section, L =

Table 1. Overview of test specimens

Test name	Geometry	Sub-number	Concrete part	Steel part	Embedded length/Contact area	Surface treatment	Number of tests	Results
Test series: SSCPOT (small-scale cube push-out tests)								
PS	Fig. 2	–1 –2 –3	Cube: 150 × 150 × 150 mm with 20 × 40 × 50 mm recess at bottom	Steel bar: 10 × 30 × 150 mm	100 mm/80 cm²	Cleaning: no Coating: no	3	Fig. 5
G	Fig. 2	–1 –2 –3	Cube: 150 × 150 × 150 mm with 20 × 40 × 50 mm recess at bottom	Steel bar: 10 × 30 × 150 mm	100 mm/80 cm²	Cleaning: no Coating: Release agent – oil	3	Fig. 5
PTFE	Fig. 2	–1 –2 –3	Cube: 150 × 150 × 150 mm with 20 × 40 × 50 mm recess at bottom	Steel bar: 10 × 30 × 150 mm	100 mm/80 cm²	Cleaning: no Coating: PTFE Teflon spray	3	Fig. 5
Test series: CoPOT (large-scale column-type push-out tests)								
0v2	Fig. 3	–1 –2	Reinforced concrete block: 340 × 1000 × 450 mm with 160 × 340 × 100 mm recess at bottom	Steel section: HEB120 L=550 mm	350 mm/2401 cm²	Cleaning: no Coating: Release agent – oil	2	Fig. 8

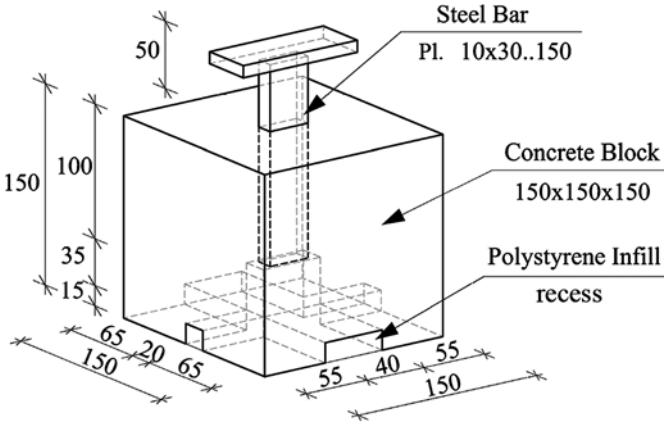

Fig. 2. Geometry of SSCPOT specimens

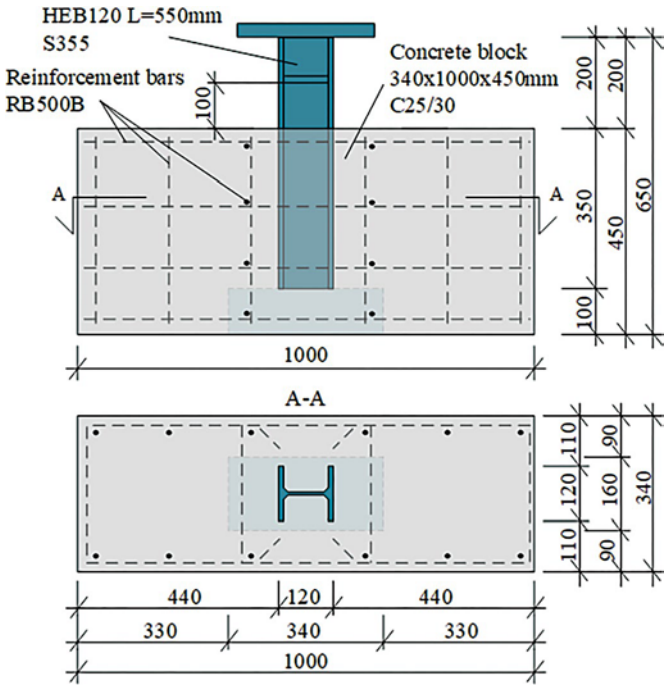

Fig. 3. Geometry of CoPOT specimens

550 mm, and a reinforced concrete block with dimensions of 340 × 1000 × 450 mm. The embedded length of the steel profile was 350 mm. In both cases, the steel surface treatment process was identical – no cleaning process had been carried out beforehand and the steel profile was coated with an anti-adhesive release oil, as in the G series of SSCPOT. The geometry of the specimens is shown in Fig. 3.

The reinforcement of each specimen was identical and comprised three types of bar: 1) longitudinal bars, 12 ∅10, L = 380 mm, 2) transverse stirrups, 4 ∅12, L = 2615 mm, and 3) U-bars around the steel section, 8 ∅12, L = 525 mm, see Fig. 3.

All characteristic material properties for structural steel, reinforcing steel and concrete were obtained experimentally according to normative testing procedures described in ISO 6892-1:2009 [17], ISO 6935-2:2007 [18] and EN 12390-3:2001 [19] respectively. The structural steel grade was S355JR+M and the measured properties were: yield strength = 455 MPa, tensile strength = 527 MPa, elastic modulus = 208 GPa and elongation at fracture = 26.5 %. The steel reinforcement grade was RB500B and the measured properties were: yield strength = 565 MPa, tensile strength = 665 MPa, elastic modulus = 206 GPa and elongation at fracture = 29 %. The manufacturer's certificate received upon delivery confirmed the concrete properties and the measured mean compression strengths after 28 days were 41 MPa for the cylinders and 45 MPa for the cubes.

3 SSCPOT – fabrication, testing and results

Securing the precise vertical orientation of the embedded steel bar, as shown in Fig. 2, was a key point during the fabrication process. A special fixing prevented the steel bars from moving during concreting. The steel parts were not cleaned in any way beforehand.

In the PS series (see Table 1), no bond-reducing coating was applied, and this represents the reference tests. The bond-reducing product applied in the G series was a high-performance anti-adhesive release agent "WETCAST – FormFluid HP" made by the Hebau company, and in the PTFE series was a PTFE spray from the KimTec company, which forms a solid coating after curing. Using a paintbrush, the steel bars of the G series were given a generous coating of the oil approx. 4 h before concreting, whereas the PTFE coating was applied uniformly with a sprayer (1–2 layers. approx. 25–40 µm) the day before concreting.

A Zwick Roell testing machine with 400 kN nominal capacity was used to perform the push-out tests (type 065146.100, series No. 807289/02). The test setup is shown in Fig. 4. The load was applied to the top of the steel bar in the form of a ramp in displacement control mode. The loading rate in the first phase was defined as 0.2 mm/min (machine travel) until reaching a force level of 20 kN. After this point, the rate was increased to 0.5 mm/min. The tests were stopped when the force dropped more than 10 % below the peak load.

The small scale of the SSCPOT specimens does not allow the inclusion of linear variable transducers to measure the relative slip between steel bar and concrete block. Consequently, the displacement and corresponding load of the machine were recorded during testing. Owing to the large stiffness of the testing machine and the small loads, the displacement of the machine was set equal to the relative slip between the steel and concrete parts of the test specimens. Any errors in the recorded data of the measured relative slip and corresponding load has been taken into account by correction displacements in the function of the imposed load obtained from the compliance test of the machine.

All test series showed similarities but also significant differences in the load-slip behaviour. In the initial phase, a

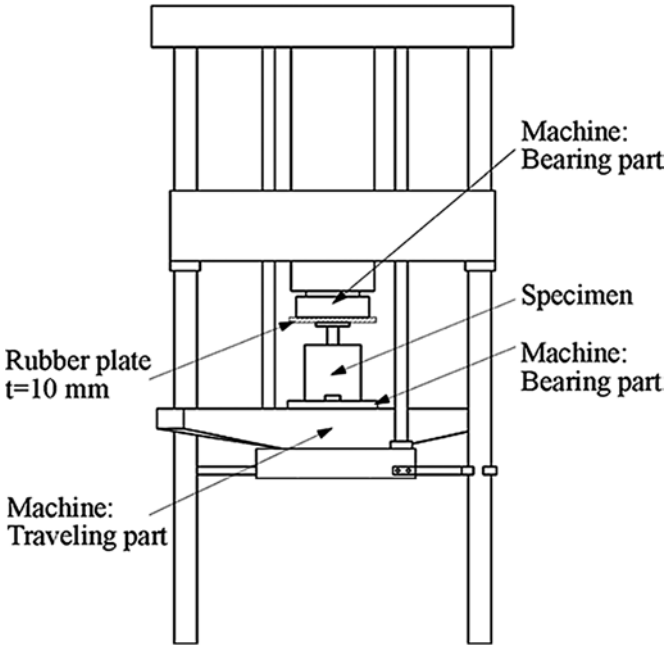

Fig. 4. SSCPOT setup scheme

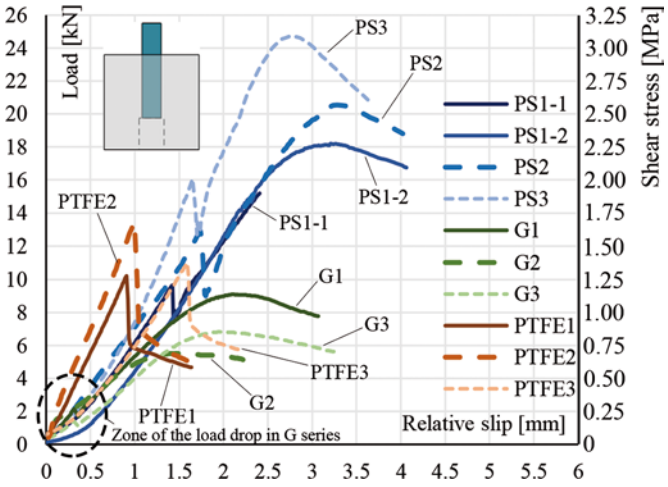

Fig. 5. Experimental SSCPOT load-slip curves

nearly linear-elastic behaviour was observed, with a sudden load drop at different points for all specimens, whereas for the G series, the load drop was barely visible and occurred at the relative slip level of approx. 0.5 mm, as shown in Fig. 5. This drop is explained by a steel-concrete adhesive chemical debonding. In the second phase, after the drop, the shear resistance of the PS and G series increases again, going beyond the first peak load due to the friction between the steel and concrete materials. However, in the PTFE series, the load increase after debonding did not occur. The third phase is considered to be after reaching the maximum load, where the load decreased with increasing slip similarly for all the tests. The slopes of the descending branches showed a certain level of ductility, which proved the existence of surface roughness friction. The load-slip responses obtained experimentally are presented in Fig. 5. A summary of the results is given in Table 2.

4 CoPOT – fabrication, testing and results

The two column-type push-out test (CoPOT) specimens, as described in row 0v2 of Table 1, were assembled from three main parts: i) the HEB120 steel sections, ii) the reinforcement cages and iii) the C25/30 concrete blocks. No surface cleaning processes were applied to the steel

Table 2. SSCPOT results summary

Value	Unit	Untreated surface				Anti-adhesive oil-treated surface				Teflon spray-treated surface			
		PS1	PS2	PS3	mean	G1	G2	G3	mean	PTFE1	PTFE2	PTFE3	mean
F_u	[kN]	18.32	20.58	24.74	21.21	9.12	5.53	6.89	7.18	10.39	13.65	11.18	11.74
F_{adh}	[kN]	9.79	13.10	16.22	13.04	2.24	1.51	1.48	1.74	10.39	13.65	11.18	11.74
δ_u	[mm]	3.20	3.27	2.79	3.09	2.15	1.47	2.19	1.94	0.92	1.00	1.60	1.18
δ_{adh}	[mm]	1.43	1.75	1.66	1.61	0.33	0.12	0.32	0.26	0.92	1.00	1.60	1.18
δ_1	[mm]	2.53	2.79	2.36	2.56	1.64	1.03	1.53	1.40	0.83	0.91	1.48	1.07
δ_2	[mm]	4.22	4.14	3.35	3.90	2.80	2.64	2.79	2.74	0.93	1.02	1.62	1.19
$\frac{\delta_2 - \delta_u}{\delta_u - \delta_1}$	[–]	1.52	1.80	1.29	1.53	1.27	2.64	0.92	1.61	0.13	0.17	0.14	0.15
K_{adh}	[kN/mm]	6.85	7.44	9.76	8.02	6.86	13.42	4.64	8.31	11.31	13.59	6.97	10.62
K_1	[kN/mm]	6.19	7.16	7.42	6.92	5.34	4.89	3.99	4.74	11.31	13.59	5.96	10.29

F_u ultimate load
F_{adh} load level at adhesion mechanism failure
δ_u relative slip corresponding to ultimate load level
δ_{adh} relative slip corresponding to adhesion failure load level
δ_1 relative slip at 0.9 F_u, before failure
δ_2 relative slip at 0.9 F_u, after failure
K_{adh} stiffness measured at δ_{adh}
K_1 stiffness measured at relative slip level of 1 mm (for PTFE, one specimen measured at δ_u)

Table 3. Measuring equipment for CoPOT – strain gauges

Strain gauges placement scheme	No.	Sensor name	Position
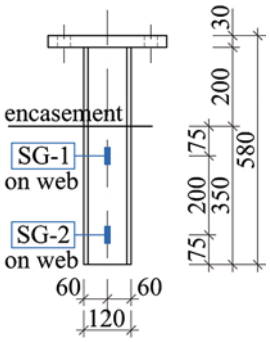	1.	SG-1	Web of steel profile – top
	2.	SG-2	Web of steel profile – bottom

profiles. A coating with the same anti-adhesive release agent WETCAST FormFluid HP, as for the SSCPOT specimens of series G, was applied to both specimens. Special care was taken during the fabrication process to ensure verticality of the steel profile.

All CoPOTs were instrumented with a set of 13 displacement transducers (DT) and a set of two strain gauges (SG) glued to the steel profiles as shown in Fig. 6 and Table 3. To measure the relative slip between the steel profile and the concrete block, two DTs were fixed with plastic clamps to the supporting bars welded to the steel profile. The aforementioned DTs were pointed towards the top surface of the concrete, see Fig. 6, DT-2 and DT-3. The reference point of displacement transducers DT-1, DT-12 and DT-13 was the ground, and they were used to measure the relative displacement between the bottom part of the steel profile and the concrete block in order to eliminate eventual deformation of the supporting frame.

The CoPOTs were executed with a hydraulic press with 1 MN nominal capacity. The test setup was identical in both cases, see Fig. 7. The test procedure of EN 1994-1-1:2004, annex B [11], was applied. The tests were conducted with displacement control and the increments were in

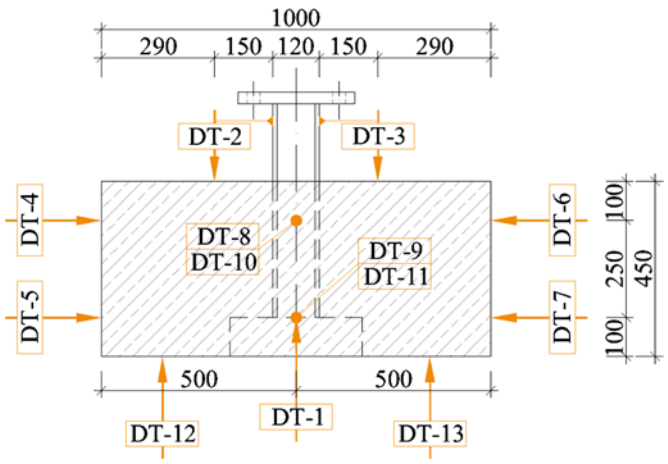

Fig. 6. Scheme of displacement transducers implemented in CoPOTs, view on south face

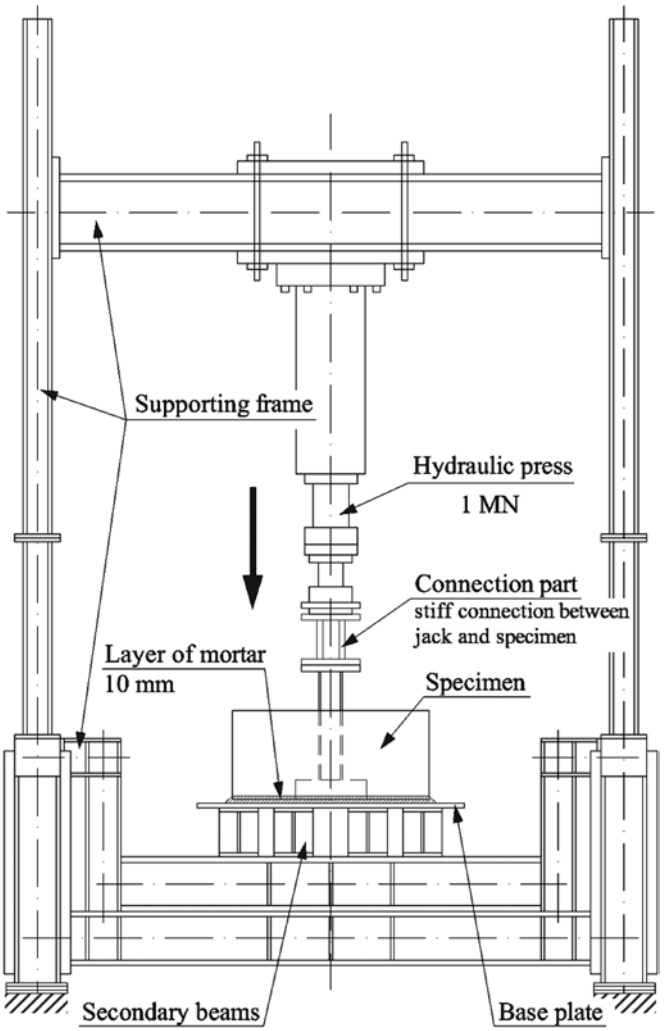

Fig. 7. CoPOT setup scheme

progressive steps. The displacement rate was set to 0.5 mm/min at the hydraulic press. A pause of 4–5 min was imposed between each load increment (approx. 30 kN) in order to allow for concrete relaxation and the investigation of the load drop characteristic. After reaching 45 % of the expected ultimate load, the specimens were subjected to 25 cycles between 5 and 40 % of the expected ultimate load with a frequency of 0.015 Hz in force control mode. After these load cycles, the quasi-static increments were continued up to failure of the specimen. After the maximum load was reached, the specimen was continuously loaded with a constant displacement up to approx. 45 mm relative slip.

The recorded data has been post-processed and the load-slip diagram is shown in Fig. 8. The slip shown is evaluated as the average signal of sensors DT-2 and DT-3, see Fig. 6. The characteristic values are summarised in Table 4.

Examination of the test specimens revealed no visual concrete damage. After reaching the ultimate load, the adhesive part of the force transfer started to decrease and only the inelastic surface roughness friction between two parts remained active.

Table 4. CoPOT experimental test results

Value	Unit	Specimen 0v2 series		Mean
		0v2-1	0v2-2	
F_u, ultimate load (peak load)	[kN]	221	194	208
F_6, load level at 6 mm of relative slip	[kN]	182	182	182
δ_u, relative slip at ultimate load	[mm]	1.49	1.64	1.56
δ_1, relative slip at 0.9 F_u, before failure	[mm]	0.52	0.93	0.72
δ_2, relative slip at 0.9 F_u, after failure	[mm]	3.43	6.95	5.19
$\frac{\delta_2 - \delta_u}{\delta_u - \delta_1}$	[–]	2.00	7.48	4.74
K_1, bond stiffness at $\delta = 1$ mm	[kN/mm]	216	178	197

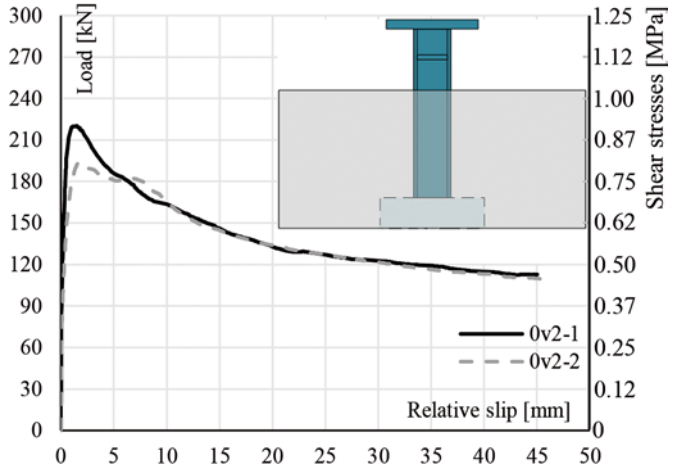

Fig. 8. CoPOT experimental load-slip curves

Based on the analysis of the measurements recorded by the strain gauges (SG) during the CoPOTs, a nearly linear distribution of the stresses over the height of the embedded steel profiles can be assumed, see Fig. 9b. In turn, that can lead to the simplified assumption that the shear stresses at the steel-concrete interface are uniformly distributed over the whole contact area. The results at the stage before the failure of the specimen have been compared with other tests found in the literature and similar conclusions have been presented by Roeder et al. [3].

The evaluation of the test results showed that all three mechanisms of the steel-concrete bond have been activated. In the initial test phase, the forces at the interface were transferred by the chemical adhesion phenomenon. This branch of the load-slip curve is characterized by a high stiffness and a nearly linear behaviour. This corresponds well to the theoretical model according to the traction-separation law of fracture mechanics, as described, for example, in *fib* Bulletin 72 [20]. A smoothed character of the load-slip curves was observed near ultimate load, which indicates a certain ductility and is in clear contradiction to the brittle behaviour of an adhesive failure. This effect can be explained by the activation of the Coulomb friction mechanism.

According to Schlaich [21], the eccentricity e of the support conditions, as indicated in Fig. 9a, allows for development of transverse compression in the system, which creates two general zones, compression and tension, to balance the internal forces. Consequently, as loading force increases, so the compression in zone 1 increases the pressure on the surface between the concrete and the steel and proportionally increases the Coulomb friction force. At the maximum load, the shear force is composed of adhesion and Coulomb friction forces. Based on the above, it was possible to conclude that the imposed boundary conditions and size of the eccentricity of the support conditions have a direct impact on the ultimate bond shear resistance. Analysis of the load-slip response given in Fig. 8 shows that the bond damage

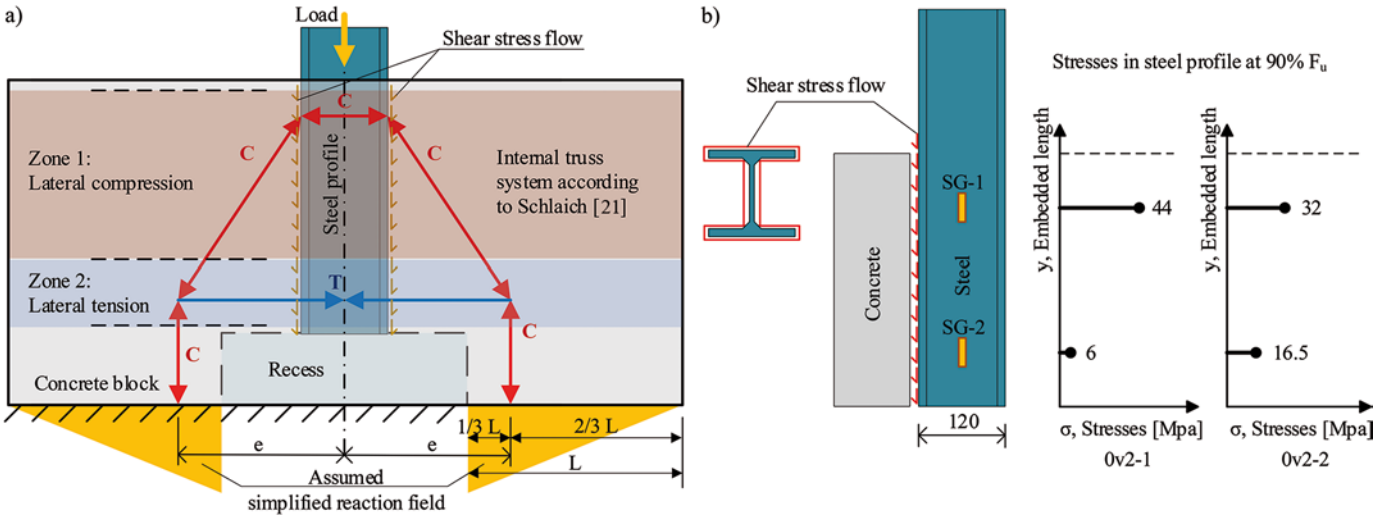

Fig. 9. CoPOT force transfer mechanism: a) simplified strut-and-tie model and b) stresses measured within steel profile

and the shear connection failure do not occur in a brittle manner, but are smoothed over the progressing relative slip. This can be explained by the fact that the adhesion failure does not occur at the same time over the total embedded length of the steel profile. The adhesive bond failure starts in the lower part of the steel profile where the lateral tension has developed, zone 2 in Fig. 9a, and progresses upwards. Consequently, with a diminishing adhesion part of the bond along the steel-concrete interface, the Coulomb friction force drops due to the reduced transverse compression in zone 1. After the peak load is reached, the adhesion part of the bond vanishes and the shear transfer at the interface is only composed of the remaining Coulomb friction part and the surface roughness friction part. The descending branches of the load-slip curves beyond a displacement of 5 mm indicate that even the surface roughness friction part of the shear resistance is not constant, instead depends on and decreases with the increasing displacement towards a constant value.

5 Evaluation of test results

As mentioned above, the steel-concrete bond is defined as the tangential shear resistance due to the chemical adhesion and friction phenomena at the steel-concrete interface. A relation between the force acting on a specified contact area and the resulting shear stresses can be defined by Eq. (1), with the simplified assumption – based on the observations given in Fig. 9b – of an equal shear stress distribution over the whole contact area of the profile. The effective steel-concrete contact area is defined by Eq. (2).

$$\tau_{\mathrm{surf,i}} = \frac{F_{\mathrm{i}}}{A_{\mathrm{c,eff}}} \left[kN/\mathrm{cm}^2 \right] \tag{1}$$

$$A_{\mathrm{c,eff}} = L_{\mathrm{emb,s}} \cdot u_{\mathrm{s,eff}} \left[\mathrm{cm}^2 \right] \tag{2}$$

where:

$L_{\mathrm{emb,s}}$ embedded length of steel part (100mm for SSCPOT and 350 mm for CoPOT)

$u_{\mathrm{s,eff}}$ effective embedded perimeter of steel part (80 mm for SSCPOT and 686 mm for CoPOT)

The effective contact area was 80 cm^2 for the SSCPOT series and 2401 cm^2 for the CoPOT series. The effective areas and ultimate loads of the experimental tests allow the calculation of the steel-concrete bond strength values according to Eq. (1). The results obtained are summarized in Table 5.

6 Comparison of results with literature data

Additional data regarding the bond strength between steel and concrete and the influence of different parameters has been found in the literature. The data are summarized in Table 6.

Based on the tests conducted and the literature review [1]–[10], it can be stated that the steel-concrete bond is sensitive to various parameters such as steel surface treatment, concrete cover thickness, level of concrete confinement, specimen geometry, boundary conditions or time. Therefore, the bond strength values cannot be directly extrapolated to specimens with different geometries and conditions. In addition, the contribution of the steel-concrete bond is significant in the force transfer mechanism of shear connectors in push-out tests with embedded steel profiles (even for greased surfaces) and cannot be disregarded. The influence of the most important parameters is discussed below.

6.1 Influence of steel surface treatment

The steel surface treatment has the most critical influence on the steel-concrete bond strength. It was observed that the specimens with rusted steel surfaces achieved the highest bond strength, see Table 6, No. 7. Furthermore, specimens with surface failure scale from the rolling process exhibited a higher resistance than specimens with cleaned steel surfaces (sandblasted or paint thinners), see Table 5, No. 1, and Table 6, No. 3. The poorest resistance properties were noticed in specimens with "greased" steel surfaces, but the values were still significant, see Table 5, No. 2. Paint or Teflon coatings (similar bond strength-reducing properties) were not as efficient in reducing the bond strength as the greasing process, see Table 5, No. 3, and Table 6, No. 7.

6.2 Influence of concrete cover

Concrete cover was the parameter with the second-largest impact on the bond strength. A thin concrete cover (approx. 50 mm) and a large steel-to-concrete surface ratio in a composite cross-section resulted in a bond with a weak shear resistance, see Table 6, No. 3 or 4. At the same time, specimens with a thick concrete cover (> 100 mm) and a small steel-to-concrete surface ratio in a composite cross-section reached high bond stress values, see Table 6, No. 6. Concrete shrinkage can have a positive or negative influence on the steel-concrete bond strength depending on the geometry of the specimen (embedded or concrete-filled steel sections) or if shrinkage creates tension or compression orthogonal to the contact surface, see Table 6, No. 1.

6.3 Influence of concrete confinement

Concrete confinement affects the frictional behaviour of the steel-concrete bond. The greater the confinement of the concrete, the higher is the shear resistance at the steel-concrete interface, see Table 6, No. 5. A large impact on the resulting bond strength values was observed when a lateral pressure acted on the interface, e.g. transverse reinforcement anchoring tensile forces from compression

Table 5. Steel-concrete bond strength comparison

No.	Specimen and steel section	Concrete	Surface treatment	Confinement	Embed. length	Effective area	Bond strength
SSCPOT							
1.	3× PS Steel bar 10×30×150	C35/45 cube 150×150×150 Age: 21 days	No	Concrete cover: c_x = 70 mm, c_y = 60 mm	100 mm	80 cm^2	2.65 MPa
2.	3× G Steel bar 10×30×150		Anti-adhesive release agent (oil)				0.90 MPa
3.	3× PTFE Steel bar 10×30×150		Teflon spray cover approx. 25–40 µm				1.47 MPa
CoPOT							
4.	2× 0v2 HEB 120 L = 550 mm	340×1000×450 f_{cm} = 41 MPa Age: 28 days	Anti-adhesive release agent (demoulding oil agent)	Concrete cover: c_x = 440 mm, c_y = 110 mm Stirrups: ∅12/117	350 mm	2401 cm^2	0.87 MPa

For a more detailed list and analysis of the steel-concrete bond, please consult the PhD thesis of the author [22]

Table 6. Steel-concrete bond – literature data

No.	Specimen and steel section	Concrete	Surface treatment	Confinement	Embed. length	Effective area	Bond strength
Roik [1]							
1.	84 specimens on rectangular and circular steel tubes Rectangular D120–140 Circular ∅120–140	Tube infill f_c = 53.4–72.4 MPa Age: 34–598 days	Surface cleaned with paint thinners. Some tests without information + interface damaged by shrinkage.	External tube cover rectangular circular	120–280 mm	529–1170 cm^2	*0.82–1.66 MPa (one series with 0.12 MPa)
2.	9 specimens on HEB200 embedded steel sections L = 500 mm	B25/35 block 330×330×470 Age: 31 days	Surface cleaned with paint thinners. Some tests coated with rust-preventive paint, thickness 25–60 µm.	Concrete cover 65 mm thick. Q131 mesh: ∅5/150	440 mm	5060 cm^2	0.7–1.40 MPa
3.	16 specimens on embedded steel plate 16×300×300	B25/35 block 75–256 mm thick 400×400 mm Age: 99 days	Mechanically cleaned. Surface cleaned with paint thinners. No coating.	Concrete cover Dir. 1: 50 mm Dir. 2: 30–120 mm Stirrups: ∅6–8/37–150	300 mm	1896 cm^2	0.45–1.06 MPa
Wium [2]							
4.	29 specimens on embedded steel sections HEB200, L = 500 mm ~HEB200, L = 1120 mm ~HEB400, L = 1270 mm	Block between 330×330×470 and ~600×500×1150 f_c = 36.5–44.1 MPa Age: 28–169 days	Sandblasted Sa2.5 (Some specimens closed at the base by endplate – no free relative slip possible.)	Concrete cover Dir. 1: 50–100 mm Dir. 2: 50–100 mm Stirrups: ∅8/100 (one series ∅8/50)	440 mm ~1000–1150 mm	5060 cm^2 ~11500–22 195 cm^2	0.54–1.20 MPa ~0.32–1.40 MPa

Table 6. Continued

No.	Specimen and steel section	Concrete	Surface treatment	Confinement	Embed. length	Effective area	Bond strength
Roeder et al. [3]							
5.	14 specimens on embedded steel sections W10×45 L = 750–1675 mm W10×22 L = 1220 mm W10×77 L = 1270 mm	Circ. column ∅500 and encasement 450×450 f_c = 35 MPa Age: 28 days	Blast cleaned to remove mill scale, cleaned with degreaser trisodium phosphate	Concrete cover Dir. 1: 90–122 mm Dir. 2: 96–152 mm Stirrups: ∅3/200, ∅3/75 Spiral: ∅3/75	600–1525 mm	7861–19978 cm^2	Average: 0.88–1.32 MPa Local: 2.20–2.75 MPa
Xing et al. [4]							
6.	18 specimens on embedded steel bars: ∅8 L = 550 mm, ∅14 L = 550 mm, ∅16 L = 550 mm	Cube 200 mm f_c = 40.8–48.5 MPa Age: 28 days	No	Concrete cover 92–96 mm	80–160 mm	20–80 cm^2	2.22–5.51 MPa (one series with 0.25 MPa)
SmartCoCo [5]							
7.	2 specimens on HEB120 embedded steel sections L = 1100 mm	C40/50 block 340×1000×1000 f_c = 71 MPa Age: 28 days	Variant 1: rusted profile Variant 2: paint coating	Concrete cover Dir. 1: 440 mm Dir. 2: 110 mm Stirrups: ∅12/150	900 mm	6174 cm^2	1.34 MPa (paint) 2.91 MPa (rust)
Tao et al. [6]							
8.	20 concrete-filled tubes, circular and rectangular sections Rectangular D120–600 Circular ∅120–400	Tube infill f_c = 42–81.8 MPa Age: 31–1176 days	For carbon steel: untreated surface For stainless steel: 2B and 2K finishing (EN10088-4:2009 [23])	External tube cover rectangular circular	600–1800 mm	2111–41760 cm^2	0.42–1.85 MPa (some series 0.03–0.33 MPa)
Pecce et al. [7]							
9.	14 partially embedded HEB180, L = 630 mm	Partial embed. f_c = 22–35 MPa Age: no information	Untreated and oiled	Space between flanges of steel profile	450 mm	2990 cm^2	0.05–0.45 MPa (flange contact only 0.1–0.75 MPa)
Xu et al. [8]							
10.	7 concrete-filled rectangular tubes, D180 and L = 600 mm	Tube infill Expansive mix f_c: no information Age: 33 days	No information	External tube cover	580 mm	3990 cm^2	0.36–0.55 MPa
Nardin et al. [9]							
11.	1 concrete-filled rectangular tube, D200 and L = 425 mm	Tube infill f_c = 48 MPa Age: no information	No information	External tube cover	375 mm	2811 cm^2	0.22 MPa
Mollazadeh [10]							
12.	5 concrete-filled rectangular tubes, D150 and L = 250–500 mm	Tube infill f_c = 29–32 MPa Age: 28 days	Cleaned with alcohol	External tube cover	200 mm and 450 mm	1120 cm^2 and 2520 cm^2	0.20–0.26 MPa

* Some results disturbed by a plastic deformation of the specimens applied beforehand – reused specimens after creep and shrinkage test of composite columns (see [1]).

~ Author refers to the chemical debonding stress values evaluated (values without friction mechanism) and no raw data available. Moreover, free slip prevented – specimen closed by end-plate. Given values approximated from diagram (see [2]).

struts, such as in push-out tests on shear connectors. The existence of transverse reinforcement without imposing a lateral pressure has a minor effect on the steel-concrete bond.

6.4 Influence of steel section geometry

The geometry of the steel section has an impact on the concrete confinement level and confinement zones, e.g. zones between flanges of H-shaped steel sections or concrete-filled tube specimens. Thus, an impact on the bond strength values is noticeable. It was observed that the steel-concrete bond strength (stress value) decreases as the scale of the steel sections used increases, see Table 5 and Table 6, No. 4.

6.5 Influence of time

In tests performed by Wium [2] it was observed that the steel-concrete bond was affected by the age of the specimen. The difference between two nominally identical specimens, tested six months apart, resulted in the bond values being reduced by approx. 15 %. This effect should be associated with creep and shrinkage effects, but is not investigated further in this article.

7 Summary and conclusions

This article describes the steel-concrete bond phenomenon between the plain steel and concrete surfaces in steel-concrete composite structures. The investigation focused on fully embedded steel sections as are used in composite columns, for instance. The impact on the bond behaviour due to the different conditions is explained. The steel-concrete bond shear strength has been evaluated from the experimental tests performed within the research project presented and compared with international findings. Good correlation was observed between the SSCPOT G series and the CoPOT series. It has been shown that the anti-adhesive release agent has a better bond-reducing property than the Teflon coating (stress reduction for the WETCAST-FormFluid HP product reached 66 % in comparison to the PS series). In the G and PTFE series, the level of the residual strength was similar. From the experimental tests executed, the ultimate bond strength values are: i) 2.65 MPa for PS series, ii) 0.9 MPa for G series, iii) 1.47 MPa for PTFE series and iv) 0.86 MPa for 0v2 series.

Moreover, it has been confirmed by results found in the literature that the steel-concrete bond strength is not a universal value and it is sensitive to different parameters. The highest values of the bond strength were noticed for the specimens with rusted steel surfaces – 2.91 MPa, SmartCoCo [5], and/or a large concrete cover (about 100 mm or more) – 5.51 MPa, Xing et al. [4]. The smallest resulting stresses were obtained for specimens with a thin concrete cover (approx. 50 mm) – 0.45 MPa, Roik [1], and with bond-reducing products applied to the cleaned steel surface – 0.12 MPa, Roik [1].

The inclusion of transverse reinforcement has a minor effect on the steel-concrete bond strength but can significantly affect the concrete confinement level and impose a lateral pressure and amplify the friction effect. Wium [2] showed that the bond strength decreases with time.

In summary, it was observed that the bond strength is very sensitive to the size of the concrete encasement, the steel surface treatment conditions, the concrete confinement level, existence of lateral forces, specimen geometry and concrete age. Therefore, the bond strength results acquired cannot be extrapolated directly to specimens with different scales and conditions. Moreover, excluding the aspect of specimen geometry, the steel-concrete bond cannot be completely eliminated by greasing the steel profile, especially not for the fully embedded steel profiles, due to irregularities on the surface of the steel profiles and the remaining chemical adhesive strength.

Acknowledgements

The MultiCoSteel research project presented is running in close collaboration with the industrial project partner ArcelorMittal Global R&D – Construction & Infrastructure Applications Department, Luxembourg. It is funded and supported by the Luxembourgish National Research Fund within the scheme of the FNR AFR-PPP PhD grant (Call 2016-1), project reference 11283614. Numerical experiments presented in this paper were carried out using the HPC facilities of the University of Luxembourg, see http://hpc.uni.lu.

References

[1] Roik, K.: *Untersuchung der Verbundwirkung zwischen Stahlprofil und Beton bei Stützenkonstruktionen*. Studiengesellschaft für Anwendungstechnik von Eisen und Stahl e.V., Düsseldorf, 1984.

[2] Wium, J. A.: *Composite Columns: Force Transfer from Steel Section to Concrete Encasement*. Thesis No. 1008 (1992), Ecole Polytechnique Federale de Lausanne, 1992.

[3] Roeder, C. W.; Chmielowski, R.; Brown, C. B.: Shear Connector Requirements for Embedded Steel Sections. *Journal of Structural Engineering* **125**(2), 1999, pp. 142–151.

[4] Xing, G.; Zhou, C.; Wu, T.; Liu, B.: Experimental Study on Bond Behaviour between Plain Reinforcing Bars and Concrete. *Advances in Materials Science and Engineering*, Vol. 2015, https://doi.org/10.1155/2015/604280.

[5] Degée, H.; Plumier, A.; Bogdan, T.; Popa, N.; Cajot, L.-G.; De Bel, J.-M.; Mengeot, P.; Hjiaj, M.; Nguyen, Q.-H.; Somja, H.; Elghazouli, A.; Bompa, D.: *Smart Composite Components – Concrete Structures Reinforced by Steel Profiles, SmartCoCo*. European Commission, Research Programme of the Research Funds for Coal & Steel, TGS 8, grant agreement RFSR-CT-2012-00031, 2016.
[6] Tao, Z.; Song, T. Y.; Uy, B.; Han, L. H.: Bond behaviour in concrete-filled steel tubes. *Journal of Constructional Steel Research* **120** (2016), pp. 81–93.
[7] Pecce, M.; Ceroni, F.: Bond tests of partially encased composite columns. *Advanced Steel Construction Journal* **6** (4), 2010, pp. 1001–1018.
[8] Xu, K.-C.; Chen, M.-C.; Yuan, F.: Confined Expansion and Bond Property of Micro-Expansive Concrete-Filled Steel Tube Columns. *The Open Civil Engineering Journal* **5** (2011), pp. 173–178.
[9] De Nardin, S.; El Debs, A. L. H. C.: Shear transfer mechanisms in composite columns: an experimental study. *Steel and Composite Structures Journal* **7** (5), 2007, pp. 377–390.
[10] Mollazadeh, M. H.: *Load Introduction into Concrete-Filled Steel Tubular Columns*. PhD thesis, University of Manchester, UK, 2015.
[11] EN 1994-1-1. Eurocode 4: Design of composite steel and concrete structures – Part 1-1: General rules and rules for buildings. European Standard, European Committee for Standardization, Brussels, Belgium, Dec 2004.
[12] Chrzanowski, M.; Odenbreit, C.; Obiala, R.; Bogdan, T.; Braun, M.; Degée, H.: Development of an innovative type of shear connector dedicated to fully embedded steel-concrete composite columns – experimental and numerical investigations. Proc. of 12th Intl. Conf. on Advances in Steel-Concrete Composite Structures (ASCCS 2018), Valencia, Spain, pp. 427–434.
[13] Chrzanowski, M.; Odenbreit, C.; Obiala, R.; Bogdan, T.: Shear stresses analysis at the steel-concrete interface with the usage of bond eliminating products. Proc. of XI Congresse de Construção Metálica e Mista (XICMM), Coimbra, Portugal, 2017, pp. 1027–1036.
[14] Goralski, C.: Zusammenwirken von Beton und Stahlprofil bei kammerbetonierten Verbundträgern. PhD dissertation, Rheinisch-Westfälischen Technischen Hochschule Aachen, 2006.
[15] EN 10025-1:2004. Hot-rolled products of structural steels – Part 1: General technical delivery conditions. European Standard, European Committee for Standardization, Brussels, Belgium, Nov 2004.
[16] EN 206-1:2000: Concrete – Part 1: Specification, performance, production and conformity. European Standard, European Committee for Standardization, Brussels, Belgium, Dec 2000.
[17] ISO 6892-1:200:. Metallic materials – Tensile testing – Part 1: Method of test at room temperature. International Standard, International Organization for Standardization, Geneva, Switzerland, 08.2009.
[18] ISO 6935-2:2007: Steel for the reinforcement of concrete – Part 2: Ribbed bars. International Standard, International Organization for Standardization, Geneva, Switzerland, 01.2007.
[19] EN 12390-3:2001: Testing hardened concrete – Part 3: Compressive strength of test specimens. European Standard, European Committee for Standardization, Brussels, Belgium, Dec 2001.
[20] *fib* Model Code for Concrete Structures 2010. International Federation for Structural Concrete (*fib*), 2013.
[21] Schlaich, J.; Schäfer, K.: Design and detailing of structural concrete using strut-and-tie models. *The Structural Engineer* **69** (6) Mar 1991, pp. 113–125.
[22] Chrzanowski, M.: Shear transfer in heavy steel-concrete composite columns with multiple encased steel profiles (working title). PhD thesis (in preparation), University of Luxembourg; proposed date of publication: Jul 2019.
[23] EN 10088-4:2009: Stainless steels – Part 4: Technical delivery conditions for sheet/plate and strip of corrosion resisting steel for construction purposes. European Standard, European Committee for Standardization, Brussels, Belgium, Apr 2009.

Authors
Maciej Chrzanowski, MSc Eng, Eng Arch
University of Luxembourg
RUES, FSTC, ArcelorMittal Chair of Steel & Façade Engineering
6, rue Richard Coudenhove-Kalergi
L-1359 Luxembourg-City, Luxembourg
maciej.chrzanowski@uni.lu

Prof. Dr.-Ing. Christoph Odenbreit
University of Luxembourg
RUES, FSTC, ArcelorMittal Chair of Steel & Façade Engineering
6, rue Richard Coudenhove-Kalergi
L-1359 Luxembourg-City, Luxembourg
christoph.odenbreit@uni.lu

Renata Obiala, PhD
ArcelorMittal Global R&D
Construction & Infrastructure Applications Dept.
66, rue de Luxembourg
L-4009 Esch-sur-Alzette, Luxembourg
renata.obiala@arcelormittal.com

Teodora Bogdan, PhD
ArcelorMittal Global R&D
Construction & Infrastructure Applications Dept.
66, rue de Luxembourg
L-4009 Esch-sur-Alzette, Luxembourg
teodora.bogdan@arcelormittal.com

Prof. Dr. Ir. Hervé Degée
Hasselt University
FET, CERG
Martelarenlaan 42
3500 Hasselt, Belgium
herve.degee@uhasselt.be